Science and Technology Infusion Climate Bulletin
NOAA's National Weather Service
39th NOAA Annual Climate Diagnostics and Prediction Workshop
St. Louis, MO, 20-23 October 2014

Assessment of the Predictability of September Sea Ice Concentration Using Sea Ice Thickness

Thomas W. Collow[1, 2], Wanqiu Wang[2], and Arun Kumar[2]

[1]*INNOVIM, LLC*

[2]*Climate Prediction Center, NCEP/NWS/NOAA*

1. Introduction

According to the 5th assessment report from the Intergovernmental Panel on Climate Change (IPCC), annual Arctic sea ice extent (SIE) is very likely (90%-100% confident) to have decreased at a rate of 0.45 to 0.51 million km^2 per decade during the 1979-2012 period due to anthropogenic influences (Vaughan et al. 2013) leading to projections of an ice free Arctic by the 2030's (Wang and Overland 2012). On a seasonal time scale, accurate sea ice prediction is important for oil and shipping interests, wildlife protection, and ecosystems management. Changes in sea ice can also influence atmospheric variability. For example, it has been observed that because Arctic sea ice melt decreases the albedo, which exacerbates the warming, there has been a faster rate of warming in the Arctic than in the lower latitudes (Kumar *et al.* 2010; Screen and Simmonds 2010). Some studies (Francis and Varvus 2012; Liu *et al.* 2012) have proposed this polar amplification in the warming trend as a mechanism for changes in the geopotential height structure and upper level jet stream pattern, which are then linked to more extreme weather events across the globe.

Blanchard-Wrigglesworth *et al.* (2011) and Wang *et al.* (2013) demonstrated that Arctic sea ice cover is potentially predictable beyond 9 months using the Community Climate System Model version 4 (CCSM4) and Climate Forecast System Version 2 (CFSv2) respectively. However, assessments also show small actual predictive skill for sea ice beyond 2-3 months (Merryfield *et al.* 2013; Wang *et al.* 2013). The difference between potential predictability and actual skill raises interesting questions for possible causes, for example, errors in the initialization of sea ice thickness. Wang *et al.* (2013) show that changes in sea ice thickness during the spring months had a large impact on forecasts of September SIE using CFSv2, with thickness increases resulting in higher SIE forecasts and vice versa, which agreed with observations. Low March 2007 sea ice thickness anomalies were cited by Kauker *et al.* (2009) as a factor leading to the record low sea ice cover the following September. Therefore, because sea ice thickness is argued to be an important predictor to forecast September sea ice cover, it is plausible that an improvement in the initial condition sea ice thickness dataset used in models could yield an improvement in September sea ice forecasts, even those initialized in the spring, narrowing the gap between prediction skill and potential predictability. However, before modeling experiments are carried out, this work aims to simply test the relationship between lagged sea ice thickness from two different datasets and September sea ice cover to assess the feasibility of such experiments.

2. Data and methods

Pan-Arctic Ice Ocean Modeling and Assimilation System (PIOMAS) monthly averaged sea ice thickness data (Zhang and Rothrock 2003) from the Polar Science Center at the University of Washington were used, in addition to Climate Forecast System Reanalysis (CFSR; Saha *et al.* 2010) sea ice thickness data from the National Centers of Environmental Prediction (NCEP). Sea ice components in both PIOMAS and CFSR assimilate satellite measurements of sea ice concentration. Sea ice thickness is derived from internal dynamics and thermodynamics without assimilating observed thickness information. Both CFSR and PIOMAS data were interpolated to 0.5° x 0.5° Arctic grid spacing. Separate time series of Arctic sea ice

Correspondence to: Thomas W. Collow, INNOVIM, LLC | Climate Prediction Center, NOAA/NWS/NCEP, 5830 University Research Court, College Park, MD; Email: Thomas.collow@noaa.gov .

volume (SIV) for each month of the period 1982-2013 were created for each dataset by multiplying the sea ice thickness of each grid cell by the respective grid cell area and taking a sum across the northern hemisphere.

First it is shown that PIOMAS sea ice thicknesses are more accurate in both magnitude and trend than CFSR data with respect to Ice, Cloud, and land Elevation Satellite (ICESat) data. Then, 2nd order polynomial detrended, lagged PIOMAS and CFSR SIV were temporally correlated with a common dataset of September SIE and sea ice area (SIA) from the National Snow and Ice Data Center which was generated with the National Aeronautics and Space Administration (NASA) Team Sea Ice Algorithm based on satellite observations (Cavalieri and Gloersen 1984), and also interpolated to a 0.5° x 0.5° grid (native NASA Team grid spacing is 25 km). The NASA Team observations have a region close to the pole that cannot be observed due to the orbit inclination of the satellites. This area, known as the polar hole, is removed from all datasets for a concise evaluation. Following the IPCC report (Vaughan *et al.* 2013), SIE is defined as the region encompassed by the edge of sea ice, represented by a concentration of at least 15%. Because of this, regions with small gaps in the sea ice with a concentration still greater than the 15% threshold are still counted as part of the SIE. SIA is different, as these gaps between sea ice are not included. For this reason SIE is always greater than SIA. In this analysis, Arctic SIE was computed by taking the cumulative sum across the northern hemisphere of the area of each grid cell with a sea ice concentration at or above 15%. SIA was calculated by multiplying the sea ice concentration in each grid cell by the area of the respective grid cell and taking a northern hemisphere sum of the results for grid cells with a sea ice concentration at or greater than 15%.

Temporal correlations were also computed on a grid point scale, using only monthly sea ice thickness and September sea ice concentration values at individual grid cells with the idea that regional patterns could exist that cannot be explained by a single hemispheric parameter like SIE or SIA. To assess the significance of the differences between the correlations, the Steiger's Z test (Steiger 1980) was employed. The test takes into account the number of data points as well as the correlation between the two datasets being compared, in this case PIOMAS and CFSR sea ice thicknesses. Because of the small size of the dataset, significance is based on an 80% confidence interval, rather than the more traditional 95%.

3. ICESat volume comparison

SIV is difficult to evaluate due to a lack of uniform observations. However, ICESat was able to provide measurements of ice thickness using a laser altimeter (Schultz *et al.* 2005). The satellite had an acquisition period each spring 2004-2008 covering roughly 35 days each, which vary slightly in their exact coverage dates. There is also a set of autumn retrievals, but because this study is concerned with prediction of September sea ice, the spring acquisition periods were of particular interest to us. For each period, from the sea ice thickness retrieved by the satellite (available from http://rkwok.jpl.nasa.gov/icesat), total SIV was calculated in the same manner as it was for PIOMAS and CFSR. The same interpolation and common mask described in the previous section was used and no detrending was applied as the time period was too short to establish any coherent trend. The ICESat data were compared with daily PIOMAS and CFSR data which were averaged to match the exact dates of the ICESat acquisition periods. Only PIOMAS and CFSR data within the ICESat domain were considered for this comparison. Figure 1 illustrates the comparison of spatial sea ice thickness and hemispheric SIV between the ICESat data and the two modeled datasets. Averaging over the spring acquisition periods, ICESat sea ice thickness patterns were closer to PIOMAS sea ice thickness patterns than to CFSR sea ice thickness patterns (Figure 1a-c). It is also apparent from Figure 1d that the ICESat SIV trends are more in line with PIOMAS trends than with CFSR trends. Root mean square errors (RMSE) relative to ICESat SIV were 2143 km^3 and 825 km^3 for CFSR and PIOMAS SIVs respectively.

4. Correlation between September sea ice cover and lagged sea ice thickness

Using detrended monthly data, no significant differences were seen in the performance of PIOMAS and CFSR when hemispheric scale SIV was correlated with September SIE and SIA over the period. However, using PIOMAS SIV showed a slightly stronger relationship with September SIA at a 1-3 month lead. Changes were more apparent on a grid point scale as there was a larger region that showed significant

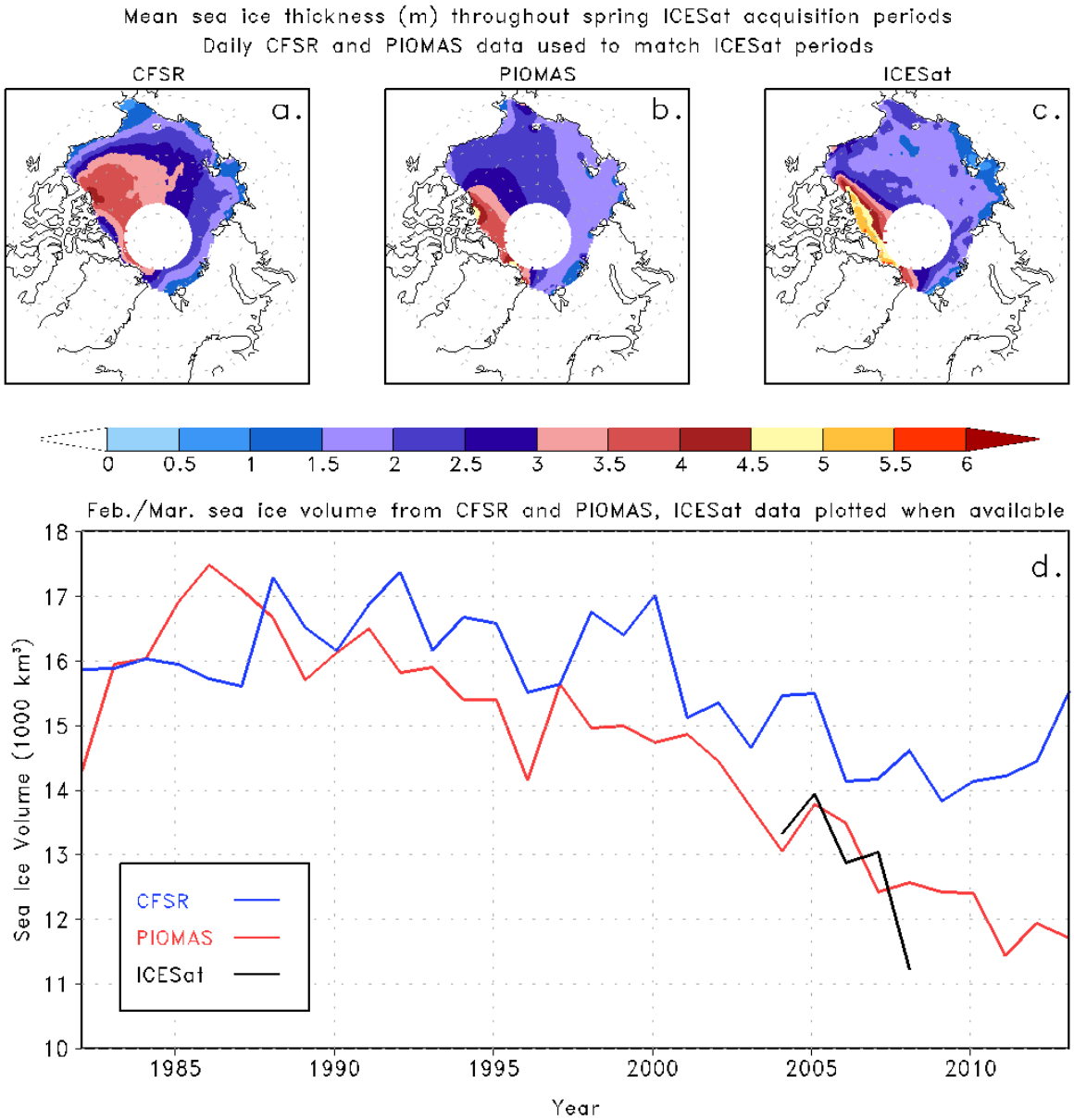

Fig. 1 Mean sea ice thickness throughout the five ICESat spring acquisition periods. Daily CFSR (panel a) and PIOMAS (panel b) data used to exactly match ICESat (panel c) periods. Panel d shows mean February-March SIV from CFSR and PIOMAS for 1982-2013 with the ICESat volume for the five acquisition periods plotted where applicable (Only grid cells common to the three datasets are used in the calculation of SIV).

increases in correlation at an 80% confidence interval than decreased skill at all lead times except zero. The area of the region with significant increases versus that with significant decreases are shown under each panel of Figure 2 and plotted as a function of lag month in panel h to further convey this point. Positive differences between increases and decreases were highest for -2 to -4 months lag (correlating May, June, or July sea ice thickness to September sea ice concentration, Figure 2c-e). Even for a lag of -6 months (March sea ice thickness, Figure 2g), increases were prevalent suggesting improvements could still be obtained out to 6 months.

5. Summary and conclusion

An assessment of the potential usefulness of PIOMAS SIV to improve the predictability of Arctic SIE and SIA in September was conducted using detrended lagged correlations. The same geographical masks

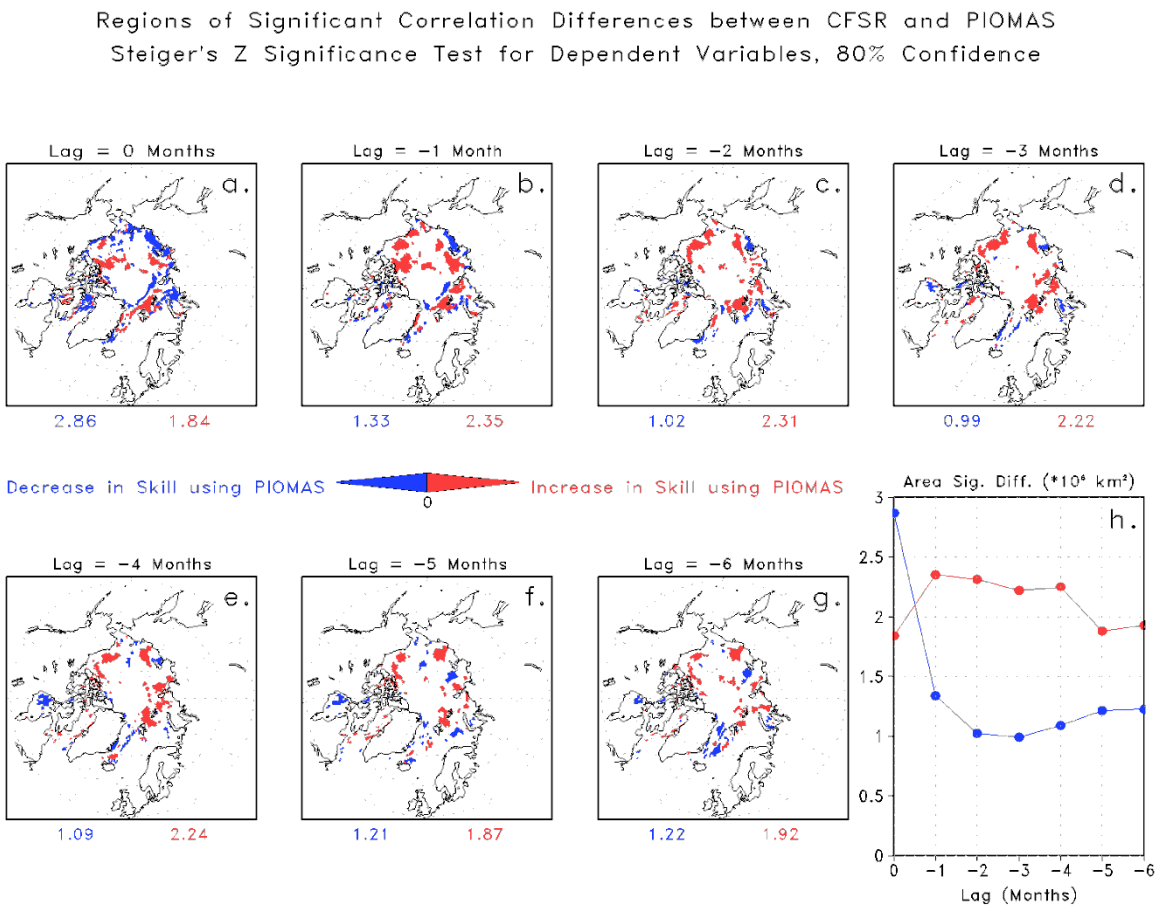

Fig. 2 Significant changes in correlation at 80% confidence that result from using PIOMAS lagged sea ice thickness to correlate with September sea ice concentration from NASA Team relative to using CFSR sea ice thickness. Red shading represents locations with a significant increase in skill using PIOMAS and blue signifies locations with a significant decrease in skill. Numbers at the bottom of each plot denote the area (10^6 km^2) of each colored region. Panels a through g are for 0 to -6 lag months. Panel h is a time series showing the area encompassed by each color (y-axis) as a function of lag month (x-axis).

were applied to all datasets to ensure consistency. Comparison with ICESat as an observational benchmark for SIV yielded PIOMAS as a more realistic dataset (within the limitation that the assessment was based on only 5 data points in time). We show that although little improvements were seen in correlating September SIE and SIA using PIOMAS SIV as opposed to CFSR SIV, significant improvements were seen when grid cell scale ice thickness and concentration were looked at. The area with significant improvements was larger than the area with significant decrease in skill in all lag months except the initial month for 80% confidence. The increase was most pronounced for correlations of May, June, and July sea ice thicknesses with the following September sea ice concentration in which the area of increase exceeded the area of decrease by a factor of near or greater than 2, which is important as this period was previously labeled as having a low predictability of September ice cover.

Because of the stronger relationship between the PIOMAS data and NASA Team observations, in addition to being more realistic as seen through comparisons with ICESat, it is plausible that utilization of PIOMAS sea ice thickness data could aid in improving prediction of September sea ice coverage, especially in the preceding June, but also as early as March. We are in the process of doing forecast experiments with the CFSv2 initialized using PIOMAS initial sea ice thickness as opposed to CFSR sea ice thickness, with the goal of producing a better sea ice forecast.

References

Blanchard-Wrigglesworth, E., C. M. Bitz, and M. M. Holland, 2011: Influence of initial conditions and climate forcing on predicting Arctic sea ice. *Geophys. Res. Lett.*, **38**, L18503, doi: 10.1029/2011GL048807.

Cavalieri, D. J., and P. Gloersen, 1984: Determination of sea ice parameters with the NIMBUS 7 SMMR. *J. Geophys. Res.*, **89(D4)**, 5355-5369.

Francis, J. A., and S. J. Varvus, 2012: Evidence linking Arctic amplification to extreme weather in mid-latitudes. *Geophys. Res. Lett.*, **39**, L06801, doi: 10.1029/2012GL051000.

Kauker, F., T. Kaminski, M. Karcher, R. Giering, R. Gerdes, and M. Voβbeck, 2009: Adjoint analysis of the 2007 all time Arctic sea-ice minimum. *Geophys. Res. Lett.*, **36**, L03707, doi :10.1029/2009GL036323.

Kumar, A., J. Perlwitz, J. Eischeid, X. Quan, T. Xu, T. Zhang, M. Hoerling, B. Jha, and W. Wang, 2010: Contribution of sea ice loss to Arctic amplification. *Geophys. Res. Lett.*, **37**, L21701, doi: 10.1029/2010GL045022.

Liu, J., J. A. Curry, H. Wang, M. Song, and R. M. Horton, 2012: Impact of declining Arctic sea ice on winter snowfall. *Proc. Natl. Acad. Sci.*, **109(11)**, 4074-4079. doi: 10.1073/ pnas. 1114910 199.

Merryfield, W. J., W.-S. Lee, W. Wang, M. Chen, and A. Kumar, 2013: Multi-system seasonal predictions of Arctic sea ice. *Geophys. Res. Lett.*, **40**, 1551-1556. doi: 10.1002/grl.50317.

Saha, S., and Co-authors, 2010: The NCEP Climate Forecast System Reanalysis. *Bull. Amer. Meteor. Soc.*, **91**, 1015-1067. doi: 10.1175/2010BAMS3001.1.

Schutz, B. E., H. J. Zwally, C. A. Shuman, D. Hancock, and J. P. DiMarzio, 2005: Overview of the ICESat Mission. *Geophys. Res. Lett.*, **32**, L21S01, doi:10.1029/2005GL024009.

Screen, J. A., and I. Simmonds, 2010: The central role of diminishing sea ice in recent Arctic temperature amplification. *Nature*, **464**, 1334-1337. doi: 10.1038/nature09051.

Steiger, J. H., 1980: Tests for comparing elements of a correlation matrix. *Psychol. Bull.*, **87(2)**, 245-251. doi: 10.1037/0033-2909.87.2.245.

Vaughan, D.G., J.C. Comiso, I. Allison, J. Carrasco, G. Kaser, R. Kwok, P. Mote, T. Murray, F. Paul, J. Ren, E. Rignot, O. Solomina, K. Steffen and T. Zhang, 2013: Observations: Cryosphere. In: Climate Change 2013: The Physical Science Basis. Contribution of Working Group I to the Fifth Assessment Report of the Intergovernmental Panel on Climate Change [Stocker, T.F., D. Qin, G.-K. Plattner, M. Tignor, S.K. Allen, J. Boschung, A. Nauels, Y. Xia, V. Bex and P.M. Midgley (eds.)]. Cambridge University Press, Cambridge, United Kingdom and New York, NY, USA, 317-382.

Wang, M., and J. E. Overland, 2012: A sea ice free summer Arctic within 30 years: An update from CMIP5 models. *Geophys. Res. Lett.*, **39**, L18501, doi: 10.1029/2012GL052868.

Wang, W., M. Chen, and A. Kumar, 2013: Seasonal prediction of Arctic sea ice extent from a coupled dynamical forecast system. *Mon. Wea. Rev.*, **141**, 1375-1394. doi: 10.1175/MWR-D-12-00057.

Zhang, J.L., and D.A. Rothrock, 2003: Modeling global sea ice with a thickness and enthalpy distribution model in generalized curvilinear coordinates. *Mon. Wea. Rev.*, **131**, 845-861.